1. Salsanabila Mariestiara PUTRI[1], 2. Indra SURJATI[2*], 3. Syah ALAM[2], 4. Yuli Kurnia NINGSIH[2], 5. Lydia SARI[2] 6. Teguh FIRMANSYAH[2], 7. Zahriladha ZAKARIA[2]
Universitas Trisakti (1), Universitas Sultan Ageng Tirtayasa (2), Universiti Teknikal Melaka Malaysia (UTeM) (3)
ORCID: 0000-0001-6944-0213*

doi:10.15199/48.2024.04.17

High Isolation of Dual-Band MIMO Microstrip Antenna with Vertical – Horizontal Configuration for 5G Communication System

Abstract. *This paper proposes dual-band MIMO microstrip antenna based on circular patch for a 5G communication system. The proposed antenna operates at a resonant frequency of 3.5 GHz and 6 GHz, using a Duroid RO5880 substrate with a dielectric constant of 2.2, a loss tan of 0.0009 and a thickness of 1.57 mm. The dual-band characteristic is obtained by placing a slot in the center of the antenna while an inset feeder is used to control the reflection coefficient. Furthermore, a high isolation coefficient is obtained by controlling the antenna configuration using vertical - horizontal. Based on the simulation results, the proposed antenna produces very good performance with a reflection coefficient of ≤ -10 dB and an isolation coefficient of ≤ -20 dB at the resonant frequency of 3.5 GHz and 6 GHz. This research is a solution for a 5G communication system that requires a dual-frequency receiving antenna that complies with high performance.*

Streszczenie. *W artykule zaproponowano dwuzakresową antenę mikropaskową MIMO opartą na patchu okrągłym dla systemu komunikacji 5G. Proponowana antena pracuje w częstotliwości rezonansowej 3,5 GHz i 6 GHz, wykorzystując podłoże Duroid RO5880 o stałej dielektrycznej 2,2, współczynniku strat 0,0009 i grubości 1,57 mm. Charakterystykę dwupasmową uzyskuje się poprzez umieszczenie szczeliny w środku anteny, natomiast wbudowany zasilacz służy do kontroli współczynnika odbicia. Ponadto wysoki współczynnik izolacji uzyskuje się poprzez sterowanie konfiguracją anteny w układzie pion - poziom. Na podstawie wyników symulacji proponowana antena charakteryzuje się bardzo dobrymi parametrami użytkowymi przy współczynniku odbicia ≤ -10 dB i współczynniku izolacji ≤ -20 dB przy częstotliwości rezonansowej 3,5 GHz i 6 GHz. Badania te dotyczą rozwiązania dla systemu komunikacji 5G, który wymaga dwuczęstotliwościowej anteny odbiorczej charakteryzującej się wysoką wydajnością. (**Wysoka izolacja dwuzakresowej anteny mikropaskowej MIMO w konfiguracji pionowo-poziomej dla systemu komunikacji 5G**)*

Keywords: 5G, MIMO, dual-band, microstrip antenna, high isolation
Słowa kluczowe: please use Google Translation.

Introduction

The technology of cellular communication has developed and entered the 5th generation (5G) stage, of course it has challenges to achieve high speed, power efficiency and system reliability [1]. Multiple Input Multiple Output (MIMO) is one of the solutions to increase the capacity of the communication system [2]. In addition, spectrum and frequency allocation is very important so that the communication system can run effectively [3]. Based on [4]–[6], one of the recommended frequencies for 5G communication systems is in the range below 6 GHz, including 3.5 GHz and 6 GHz. In addition, high performance antennas are required to be able to transmit information from transmitters and receivers, especially for 5G communication systems. MIMO antenna systems play an important role in wireless communication systems to meet the characteristics of wide bandwidth, higher data rates and limited space. One of the antennas that has been developed for the purposes of wireless communication systems is the microstrip antenna [7].

The development of microstrip antennas for 5G communication systems has been widely described in previous studies [8]–[12]. The previous research presented [13] proposed a Hairpin Filter microstrip antenna that operates for 5G telecommunications systems at a frequency of 4.45 GHz, while the proposed research [14] is a microstrip antenna with a Defected Ground Structure for 5G communications at a frequency of 3.5 GHz. The two previous studies cannot be used for MIMO communication systems because they only consist of one patch. Another study [15] proposed a 4-element MIMO array antenna for 5G communication systems at a resonant frequency of 3.5 GHz, but the isolation coefficient obtained was not optimal. Research [16] proposes MIMO antennas for 5G communication systems that are already dual-band at frequencies of 0.7 GHz and 2.3 GHz and have good isolation coefficient. However, the proposed resonant frequency does not meet the criteria and requirements of the 5G communication system regulations in Indonesia, where the recommended resonant frequencies are 3.5 GHz and 6 GHz.

Therefore, this study provides a solution by proposing a MIMO microstrip antenna which has dual-band characteristics and high isolation. The proposed antenna has a circular patch operating at f_{r1} = 3.5 GHz and f_{r2} = 6 GHz with a reflection coefficient (S_{11}) ≤ -10 dB and mutual coupling (S_{21}) ≤ -20 dB. In order to achieve dualband characteristics, the slot and inset method is proposed to control the parameter S_{11} and the resonant frequency of the antenna. Furthermore, a high isolation coefficient is obtained by controlling the antenna configuration. The main objective of this research is to produce a MIMO microstrip antenna with dual-band characteristics and high isolation value so that it can be recommended as a receiving antenna for 5G communication systems.

Antenna Design

In this paper, the proposed antenna is designed using a Duroid RO5880 substrate with a dielectric constant of 2.2, a loss tan of 0.0009 and a thickness of 1.57 mm. The antenna structure consists of a radiating element made of copper and a connector made of brass. The model development of the proposed antenna is shown in **Fig. 1**.

The first stage of this research is to design a single-element antenna based on a circular patch connected to a connector with an impedance of 50 Ohm using a microstrip channel as shown in Fig. 1 (a). The second stage is optimizing the antenna by adding an inset on the edge of the feeder and a slot in the center of the patch antenna which serves to reduce the reflection coefficient and generate dual frequencies as shown in Fig.1 (b). In this paper, the antenna is designed to operate at dual frequencies at f_{r1} = 3.5 GHz and f_{r2} = 6 GHz for 5G communication system. The third stage is to develop the proposed antenna model with 2 MIMO ports arranged vertically and separated by a distance (d) as shown in **Fig.1 (c)**. It should be noted, the distance between the two MIMO antennas will affect the isolation coefficient (S_{21}). The final

stage of antenna design is to optimize the MIMO antenna structure by rotating one of the antenna patches to be horizontal as shown in Fig. 1 **(d)**. This aims to reduce S_{21} so that the antenna has a high mutual coupling.

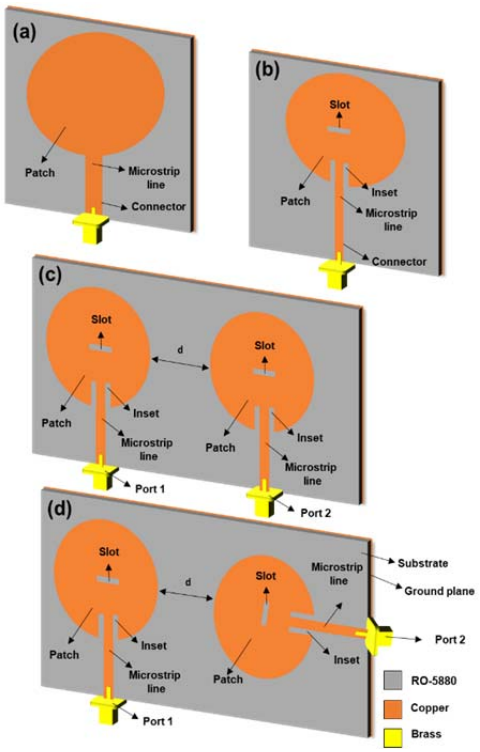

Fig. 1 Model development of the antenna; (a) single element circular patch antenna design, (b) circular patch antenna design with inset and slot, (c) 2 port MIMO antenna design with vertical configuration, (d) 2 port MIMO antenna design with vertical-horizontal configuration

The dimensions of the circular patch antenna are obtained using equations (1) and (2) where the logarithmic function will affect the dimensions of the circular patch antenna [8].

(1) $$F = \frac{8{,}791\ x10^9}{fr\sqrt{\varepsilon r}}$$

where F represents the logarithmic function, f_r represents the resonant frequency and ε_r represents the dielectric constant. Furthermore, the radius of the circular patch microstrip antenna is determined based on equation (2).

(2) $$r = a\sqrt{1} + \frac{2\,h}{\pi\,F\,\varepsilon\,r}\left[Ln\left(\frac{\pi F}{2\,h}\right)\right] + 1{,}7726$$

where r represents the radius of the circular patch antenna, h is the thickness of the substrate, π is 3,14. Furthermore, the dimensions of the width of the microstrip feed line (W_z) with an impedance value of 50 Ω are determined using equation (3) and equation (4) [17].

(3) $$B = \frac{60\,\pi^2}{Zo\sqrt{\varepsilon_{reff}}}$$

(4) $$Wz = \frac{2\,h}{\pi}\left\{B - 1 - \ln(2B-1) + \frac{\varepsilon r}{2\varepsilon r}\left[\ln(B-1) + 0{,}39 - \frac{0.61}{\varepsilon r}\right]\right\}$$

where B represents the impedance constant of the microstrip line, Z_0 is the impedance of the microstrip line, ε_{reff} is the effective dielectric constant of the microstrip line and W_z represents the width of microstrip lines. The overall dimensions of the circular patch microstrip antenna are shown in Table 1.

Table **1**. Dimension of circular patch microstrip antenna

Parameter	Dimension (mm)
r	16
W_z	2,2
L_z	17
W_g	50
L_g	50

Furthermore, the ground planes used in this paper are represented as W_g and L_g with dimensions of 50 mm x 50 mm. The circular patch microstrip antenna design is shown in Fig. 2.

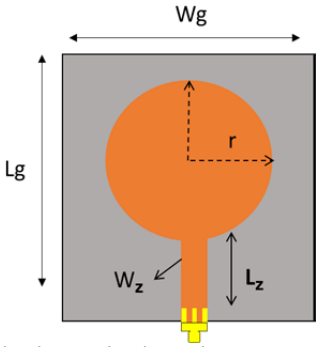

Fig. 2 Design of a circular patch microstrip antenna

The simulation and design of the proposed antenna was carried out using AWR MWO 2009 software by observing S_{11}, VSWR and gain of proposed antenna. The simulation results of the single element circular patch antenna are shown in Fig. 3(a), Fig. 3(b) and Fig. 3(c).

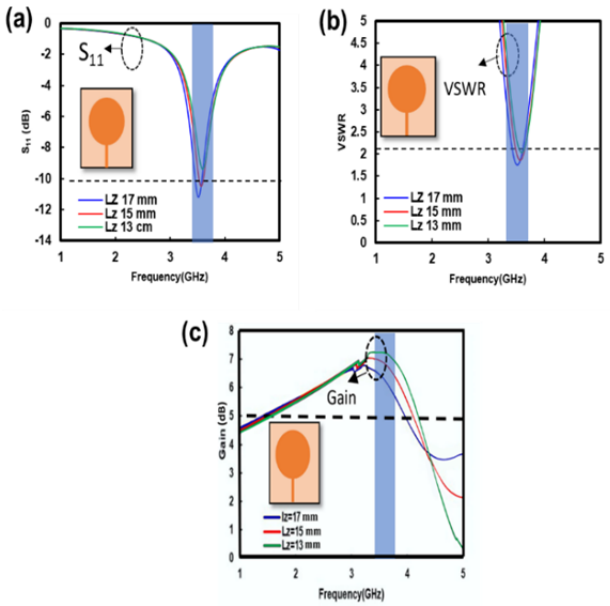

Fig. 3 Simulation results of circular microstrip patch antenna; (a) S_{11} of proposed antenna (b) VSWR of proposed antenna, (d) gain of proposed antenna

Table 2. Simulation result from iteration of L_z

Iteration	L_z (mm)	Parameters			
		S_{11} (dB)	VSWR	BW (MHz)	*Gain* (dB)
1st iteration	13	-8,73	2,37	70	7,2
2nd iteration	15	-10,03	2,05	80	6,8
3rd iteration	17	-11,21	1,77	120	6,3

Fig. 3 (a), Fig. 3 (b) and Fig. 3 (c) show that the parameters S_{11}, VSWR and gain of the single element

circular patch antenna can be controlled by changing the dimensions of L_z with a range of 13 mm – 17 mm as shown in Table 2.

Table 2 shows the best performance of the proposed antenna obtained at 3rd iteration where the antenna operates at a resonant frequency of 3.5 GHz with S_{11} of -11.21 dB, VSWR of 1.77, bandwidth of 120 MHz and gain of 6.3 dB. From the simulation results it can be seen that the antenna still works at one resonant frequency and has S_{11} and VSWR which are still not optimal, so it needs to be optimized.

In this paper, dual-band frequencies are generated using the slot technique while the reduction of the reflection coefficient of each resonant frequency is controlled using an inset feed. Furthermore, the design of single element circular patch antenna with inset and slot is shown in **Fig. 4**.

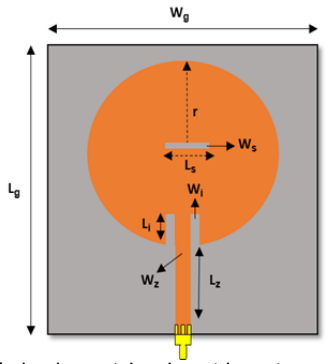

Fig. 4. Design of circular patch microstrip antenna with inset and slot

The simulation results of the circular patch antenna with inset and slot are shown in Fig. 5 (a) and Fig.5 (b) where the dimensions of the inset represented by L_i and the slot are L_s.

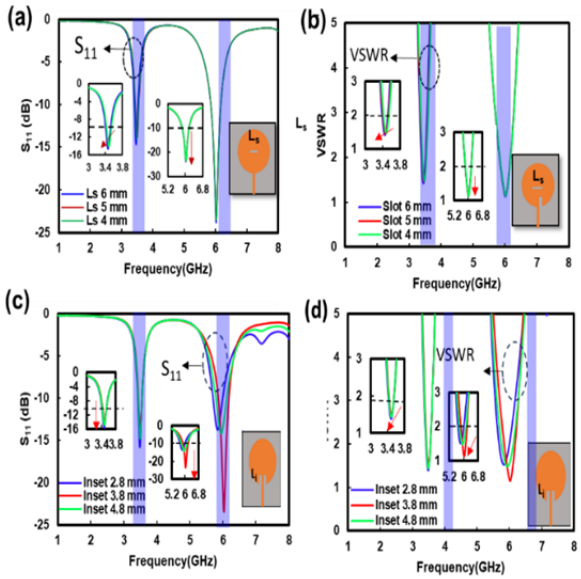

Fig. 5 Design simulation results of circular patch antenna with inset and slot (a) S_{11} circular patch antenna with slot, (b) VSWR circular patch antenna with slot, (c) S_{11} circular patch antenna with inset (c) VSWR circular patch antenna with inset.

Furthermore, Fig. 5 (a) and Fig. 5 (b) show that the parameters S_{11} and VSWR of the circular patch antenna design with inset and slot can be controlled by changing the dimensions of L_i with a range of 2.8 mm – 4.8 mm and the dimensions of the slot L_s with range 3 mm – 5mm. The overall results of the iteration process of L_i and L_s are shown in Table 3 and Table 4.

Table 3. Simulation result from iteration of L_i

Iteration	L_i (mm)	Parameters					
		S_{11} (dB)		VSWR		BW (MHz)	
		f_{r1}	f_{r2}	f_{r1}	f_{r2}	f_{r1}	f_{r2}
1st iteration	2,8	-15,73	-10,10	1,42	1,97	128	286
2nd iteration	3,8	-14,74	-14,10	1,50	1,18	121	335
3rd iteration	4,8	-13,88	-23,07	1,45	1,54	111	316

Table 4. Simulation result from iteration of L_s

Iteration	L_s (mm)	Parameters					
		S_{11} (dB)		VSWR		BW (MHz)	
		f_{r1}	f_{r2}	f_{r1}	f_{r2}	f_{r1}	f_{r2}
1st iteration	4	-13,84	-23,14	1,87	1,14	114	319
2nd iteration	5	-13,77	-23,22	1,67	1,16	110	321
3rd iteration	6	-13,84	-23,24	1,57	1,17	114	319

Table 3 shows that the addition of the inset succeeded in producing an antenna with dual frequencies where f_{r1} = 3.5 GHz and f_{r2} = 6 GHz. Furthermore, the best performance of the proposed antenna is obtained in the 3rd iteration where the antenna operates at the frequencies f_{r1} = 3.5 GHz and f_{r2} = 6 GHz with S_{11} of -13.88 dB and -23.07 dB, VSWR 1.45 and 1.54 then has a bandwidth of 111 MHz and 316 MHz with dimensions of L_i = 4.8 mm. Furthermore, Table 4 shows the optimization of the antenna by controlling the dimensions of L_s where the best performance of the proposed antenna is obtained in the 3rd iteration with L_s = 6 mm where the antenna operates at the frequency f_{r1} = 3.5 GHz and f_{r2} = 6 GHz with S_{11} of - 13.84 dB and -23.24 dB, VSWR 1.57 and 1.17, then has a bandwidth of 114 MHz and 319 MHz. From the simulation results, it can be seen that the antenna operates at two resonant frequencies and has S_{11} and VSWR which meet the standards with $S_{11} \leq$ -10 dB and VSWR ≤ 2. Therefore, the next step is to design and simulate a MIMO antenna with 2 ports.

MIMO Antenna Design

The design of a 2-port MIMO antenna with a vertical configuration is shown in **Fig. 6**.

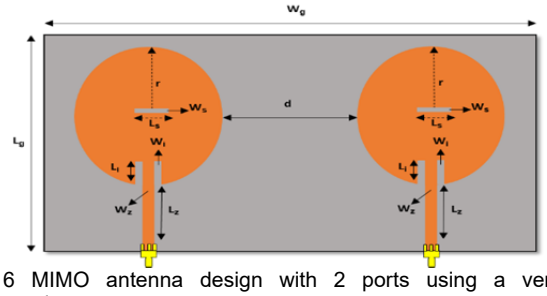

Fig. 6 MIMO antenna design with 2 ports using a vertical configuration

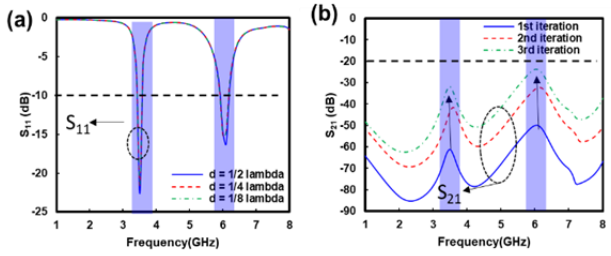

Fig 7. Simulation results of an antenna with a vertical configuration: (a) simulation of S_{11}, (b) simulation of S_{21}

The simulation results of the proposed antenna using a vertical configuration are shown in Fig. 7(a) and Fig. 7(b).

Fig.7 (a) and Fig.7 (b) show that parameter S_{11} of the antenna operating at f_{r1} = 3.5 GHz and f_{r2} = 6 GHz is ≤ -10 dB while for S_{21} of the MIMO antenna is ≤ -20 dB using vertical configuration which can be controlled by adjusting the distance between the antenna patches (d) which is determined using equation (5) as follows [8]:

$$d = \frac{1}{4}\lambda \tag{5}$$

where d represents the distance between MIMO antennas and λ is the wavelength. The overall simulation results from the iteration of the distance *(d)* with the vertical configuration are shown in Table 5.

Table 5. Simulation results from iteration of *d*

Iteration	*d* (mm)	Parameters			
		S_{11} (dB)		S_{21} (dB)	
		f_{r1}	f_{r2}	f_{r1}	f_{r2}
1st iteration	40	-22,53	-14,68	-61,11	-49,98
2nd iteration	20	-21,10	-15,02	-41,98	-32,38
3rd iteration	10	-21,10	-15,18	-31,96	-23,81

Table 5 shows the best performance obtained in the second iteration where the antenna operates at f_{r1} = 3.5 GHz and f_{r2} = 6 GHz with S_{11} of -21.10 dB and -15.02 dB and S_{21} of -41.98 dB and -32.38 dB. From the simulation results the MIMO antenna using a vertical configuration has succeeded in producing S_{21} ≤ -20 dB. Furthermore, to reduce S_{21} optimization is carried out by changing the configuration of the MIMO antenna.

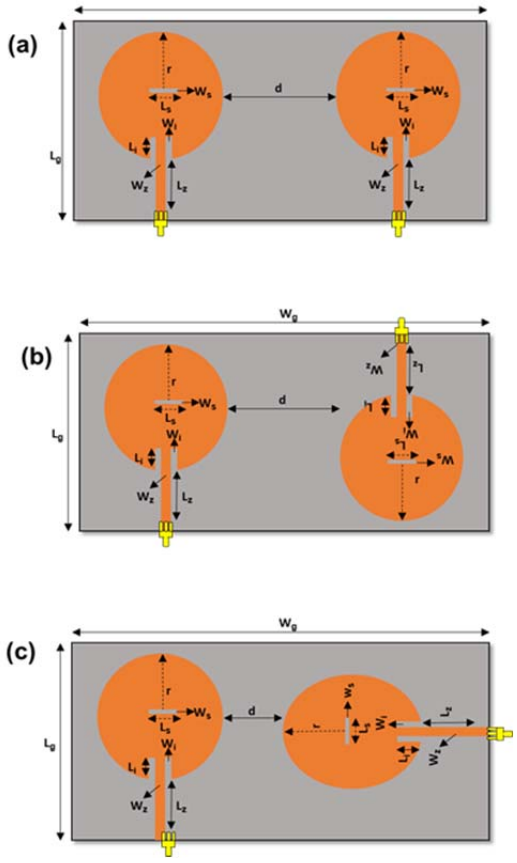

Fig. 8. Optimization design of a 2-port MIMO antenna: (a) with an angle of 0°, (b) with an angle of 180°, (c) with an angle of 90°

In this paper, optimization of the isolation coefficient parameter (S_{21}) is carried out by changing the configuration of the 2-port MIMO antenna. The mechanism used is to rotate one of the MIMO patch antennas with an angle of 90° and 180° and compare it with the initial antenna configuration with an angle 0°. Furthermore, the optimization design of the vertical-horizontal 2 port MIMO antenna is shown in **Fig.8**.

Fig. 8(a) shows the 1st iteration of the initial 2 port MIMO antenna design which uses a vertical configuration with a distance of d = 20 mm. Furthermore, the 2nd iteration is carried out by changing the configuration by rotating the MIMO patch antenna with a vertical orientation of 180° with a distance of d = 20 mm. Furthermore, the 3rd optimization is carried out by rotating the MIMO patch antenna with a vertical orientation of 90° with a distance of d = 20 mm. The purpose of this optimization is to obtain a high isolation coefficient (S_{21}). A high isolation coefficient indicates that MIMO antennas work independently so they have a low correlation and do not affect each other when operating simultaneously.

The simulation results of the optimization of the 2-port MIMO antenna design with a vertical - horizontal configuration are shown in Fig.9 (a) and Fig.9 (b).

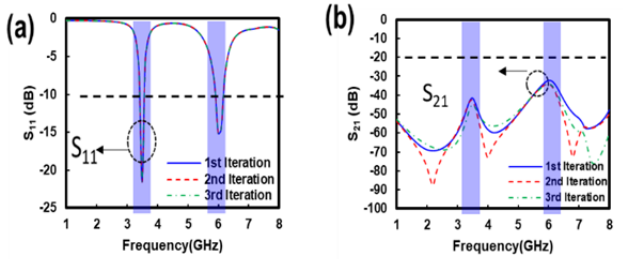

Fig. 9 Simulation result of MIMO antenna, (a) simulation result of S_{11}, (b) simulation result of S_{21}

Fig. 9 (a), Fig. 9 (b) shows that parameter S_{21} of the MIMO 2 port antenna optimization vertical - horizontal configuration can be controlled by rotating one of the MIMO patch antennas with an angle of 0°, 90° and 180°. Furthermore, the results of the entire iteration and optimization process of the configuration of the 2-port MIMO antenna is shown in Table 6.

Table 6. Simulation result from different configurations of MIMO antenna

Iteration	Parameters	
	S_{21} (dB)	
	f_{r1}	f_{r2}
1st iteration	-41,82	-32,38
2nd iteration	-43,37	-34,12
3rd iteration	-45,22	-34,28

Table 6 shows that the best performance of the 2-port MIMO antenna configuration was obtained in the 3rd iteration where S_{21} was -45.22 dB and 34.28 dB. From the simulation results, it can be concluded that the 2-port MIMO antenna in a vertical – horizontal configuration has worked at two resonance frequencies and has S_{11} ≤ -10 dB and S_{21} ≤ -20 dB. The next stage is the fabrication and measurement of the proposed antenna in the laboratory.

Measurement and Verification

The fabrication of the proposed antenna was carried out using a substrate type RO5880 with dielectric constant (ε_r) of 2.2, thickness (h) of 1.578 mm and loss tan ($tan\ \delta$) of 0.0009. The fabricated antenna is shown in Fig.10.

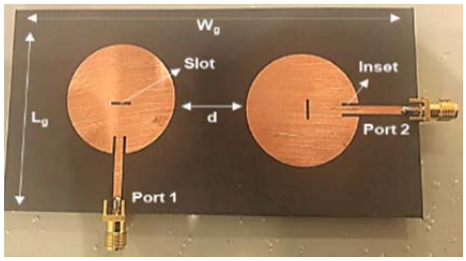

Fig 10. Fabricated proposed antenna

The measurement process was carried out using a *Vector Network Analyzer* (VNA) with a frequency range of 1 – 8 GHz with a sweep frequency of 0.01 GHz. The configuration of the measurement setup is shown in Fig. 11.

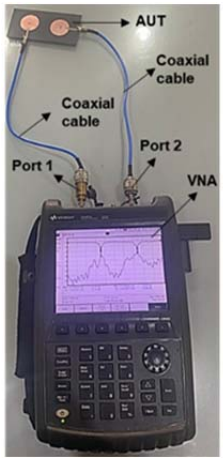

Fig 11. Measurement setup of proposed antenna

Fig.11 shows the VNA consisting of port 1 and port 2 which are connected directly to the Antenna Under Test (AUT) using a coaxial cable with an impedance of 50 Ohm. The measurement results of parameters S_{11} and S_{21} of the proposed antenna are shown on the VNA screen. The measurement results of the proposed MIMO antenna are shown in Fig. 12.

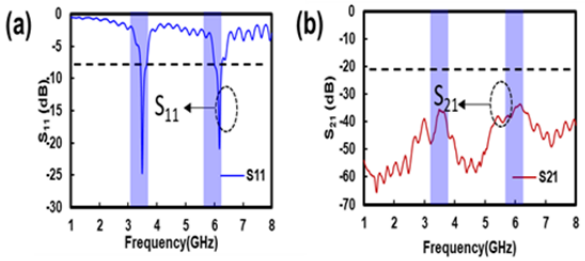

Fig 12. Measurement result of proposed antenna using VNA; (a) measurement result of S_{11}, (b) measurement result of S_{21} .

Fig.12 (a) and Fig.12 (b) shows that the parameter S_{11} of the proposed antenna at resonant frequencies of f_{r1} and f_{r2} are -24.61 dB and -20.84. Furthermore, S_{21} of proposed antena are -36.71 dB and -34.88 dB for each resonant frequency, respectively.

The next step is to validate and observe the performance of the proposed antenna. Validation was carried out by comparing the simulation and measurement results of parameters S_{11} and S_{21} of the proposed MIMO antenna. The comparison of the simulation and measurement processes of the proposed antenna are shown in Fig. 13.

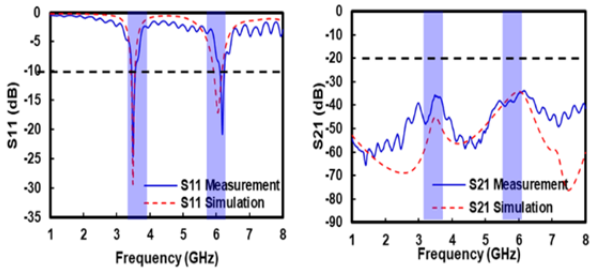

Fig. 13 Comparison of simulation and measurement, (a) comparison of S_{11}, (b) comparison of S_{21}.

Fig. 13 shows that the simulation results are in line with the measurement results. The simulation results show that the antenna operates at f_{r1} = 3.48 GHz and f_{r2} = 6.07 GHz while the measurements show that the antenna operates at f_{r1} = 3.52 GHz and f_{r2} = 6.18 GHz. This shows that there is a shift in the resonant frequency between the simulation and measurement processes of 1.15% and 1.78% for each resonant frequency. This is due to errors and inaccuracies in the fabrication process and connector installation so that the impedance of the antenna changes. Furthermore, for S_{11} from the simulation process on f_{r1} and f_{r2} obtained -29.45 dB and -17.16 dB while for the measurement process obtained -24.61 dB and -20.84 dB. This shows that the antenna meets the criteria with $S_{11} \leq$ -10 dB. Furthermore, S_{21} from the simulation process on f_{r1} and f_{r2} obtained -45.70 dB and -34.88 dB while the measurement process obtained -36.71 dB and -34.89 dB at each resonant frequency. The overall comparison results from the simulation and measurement processes are shown in **Table 7**.

Table 7. Comparison of resonant frequency of proposed antenna from simulation and measurement

Frequency (GHz)	Process		Error (%)
	Simulation	Measurement	
f_{r1}	3.48	3.52	1,15 %
f_{r2}	6.07	6.18	1,81 %

From the results shown in **Table 7** can be concluded that the designed antenna has the same characteristics for the simulation and measurement processes where the antenna has operated at two resonant frequencies with $S_{11} \leq$ -10 dB and $S_{21} \leq$ -20 dB. The next step is to evaluate the performance of the MIMO antenna by observing the *Envelope Correlation Coefficient* (ECC) and *Diversity Gain* (DG) parameters.

ECC shows the correlation between the two antennas when working together for the MIMO configuration. Generally, the ECC range used is in the range 0 - 1. Furthermore, the threshold value of the ECC that is commonly used in a MIMO antenna design is ≤ 0.5 [17]. ECC parameters can be determined using equation (6) as follows:

$$\text{ECC} = \frac{|S_{11}{}^{*}S_{12}+S_{21}{}^{*}S_{22}|^2}{(1-|S_{11}|^2-|S_{21}|^2)-(1-|S_{22}|^2-|S_{12}|^2)} \tag{6}$$

Diversity Gain (DG) describes the ability to deal with multipath fading. The DG value describes the ability to increase or maintain the signal against noise when combining all signals on the antenna rather than on one antenna. The diversity of MIMO antennas is indicated by DG ≤ 10 dB [18]. DG can be determined based on equation (7) as follows:

$$DG = 10\sqrt{1-(ECC)^2} \tag{7}$$

Fig.14 shows a comparison of the ECC and DG at the two resonant frequencies of the proposed antenna. Based on the calculation results, the ECC on f_{r1} and f_{r2} is 0.0018 and 0.0012 while for DG it is 10 dB and 9.99 dB. This shows that the ECC and DG of the designed antenna have met the target set where ECC ≤ 0.5 and DG ≤ 10 dB. From these results it can be concluded that the designed MIMO antennas have a low correlation coefficient, so they do not affect each other when working together.

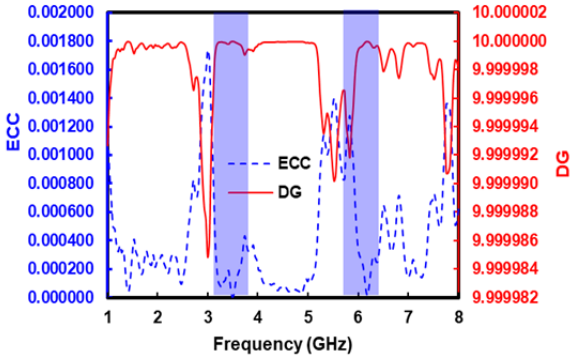

Fig. 14 ECC and DG from proposed antenna

Furthermore, the simulation results of the gain and radiation pattern of the proposed antenna are shown in Fig. 15.

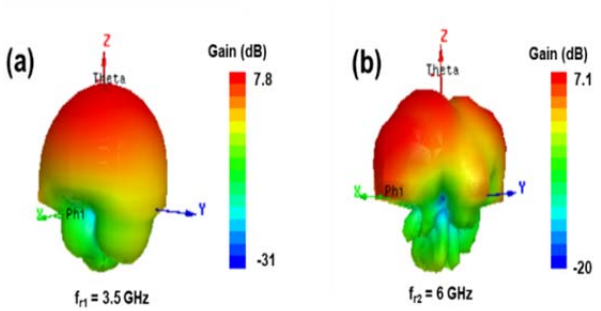

Fig. 15 Radiation pattern and gain of proposed antenna, (a) at f_{r1} = 3.5 GHz, (b) at f_{r2} = 6 GHz.

Fig. 15 (a) and Fig. 15 (b) show that the proposed antena has a maximum gain of 7.8 dB and 7.1 dB for f_{r1} = 3.48 GHz and f_{r2} = 6.18 GHz. Furthermore, Table 8 is proposed to show the novelty of this study compared to previously proposed studies.

Table 8.

Ref.	Freq. (GHz)	Paramaters				MIMO	*Dual Band*
		S_{11} (dB)	S_{21} (dB)	ECC	DG (dB)		
[13]	4.45	-45	NA	NA	NA	No	No
[15]	3.5	-14	-19.25	NA	NA	Yes	No
[14]	3.5	-17.43	NA	NA	NA	No	No
[16]	0.7 2.3	-30 -15	-31.37 -14.26	0,127 0,007	NA	Yes	Yes
This work	3.52 6.18	-24,61 -20.84	-36,71 -34.88	0,0018 0.0012	10 9.99	Yes	Yes

Table 8 shows that the proposed antenna has a novelty that can operate at two different resonance frequencies with low ECC and high DG. In addition, the proposed antenna has been configured in MIMO so that it can be recommended for 5G communication systems.

Table 8. Comparison result with previous studie

Conclusion

This paper has described the realization of a 2-port MIMO microstrip antenna with a circular patch that operates at two resonant frequencies, namely f_{r1} = 3.5 and f_{r2} = 6 GHz. The slot and inset methods are proposed to control parameter S_{11} and the resonant frequency of the antenna, while the vertical-horizontal configuration is proposed to reduce parameter S_{21}. From the measurement results it was found that S_{11} was -24.61 dB and -20.84 dB while for S_{21} it was -36.71 dB and -34.88 dB for each resonant frequency. Furthermore, the ECC was obtained, namely 0.0018 and 0.0012 and DG of 10 dB and 9.99 dB for f_{r1} and f_{r2}, respectively. From these results it can be concluded that the designed antenna meets the specified targets, namely S_{11} ≤ -10 dB, S_{21} ≤-20 dB, ECC ≤ 0.5 and DG ≤ 10 dB. This research is very useful and can be recommended as a receiving antenna for 5G communication systems.

Acknowledgements

This research is fully supported and funded by the Ministry of Education and Culture of the Republic of Indonesia and the Research and Community Service Institute of Trisakti University through a Postgraduate Research Grant for fiscal year of 2023/2023 with contract number 1440/LL3/AL.04/2023 and 703/A/LPPM/USAKTI/VII/2023.

Authors

Salsanabila Mariestiara Putri, Department of Electrical Engineering,Universitas Trisakti, Indonesia Email : 162012100004@std.trisakti.ac.id; Indra Surjati, Department of Electrical Engineering,Universitas Trisakti, Indonesia E-mail: indra@trisaktri.ac.id; Syah Alam, Department of Electrical Engineering,Universitas Trisakti, Indonesia E-mail: syah.alam@trisaktri.ac.id; Lydia Sari, Department of Electrical Engineering,Universitas Trisakti, Indonesia E-mail: lydia_sari@trisaktri.ac.id;Yuli Kurnia Ningsih, Department of Electrical Engineering,Universitas Trisakti, Indonesia E-mail: yuli_kn@trisakti.ac.id ; Teguh Firmansyah, Department of Electrical Engineering,Universitas Sultan Ageng Tirtayasa, Indonesia E-mail: teguhfirmansyah@untirta.ac.id; Zahriladha Zakaria, Fakulti Kejuruteraan Elektronik dan Kejuruteraan Komputer (FKEKK) of Universiti Teknikal Malaysia Melaka (UTeM), Malaysia Email : zahriladha@utem.edu.my

REFERENCES

[1]: A review," *IEEE Access*, vol. 7. Institute of Electrical and Electronics Engineers Inc., pp. 127276–127289, 2019. doi: 10.1109/ACCESS.2019.2938534.

[2] S. Singh, A. Kumar Singh, Karunesh, A. Pandey, and R. Singh, "A Novel MIMO Microstrip Patch Antenna for 5G Applications," in *Proceedings - IEEE 2021 International Conference on Computing, Communication, and Intelligent Sistems, ICCCIS 2021*, Institute of Electrical and Electronics Engineers Inc., Feb. 2021, pp. 828–833. doi: 10.1109/ICCCIS51004.2021.9397137.

[3] S. Parkvall, E. Dahlman, A. Furuskar, and M. Frenne, "NR: The new 5G radio access technology," *IEEE Communications Standards Magazine*, vol. 1, no. 4, pp. 24–30, Dec. 2017, doi: 10.1109/MCOMSTD.2017.1700042.

[4] A. S. Mirfananda and M. Suryanegara, "5G spectrum candidates beyond 6 GHz: A simulation of Jakarta environment," *Proc. - 2016 IEEE Reg. 10 Symp. TENSYMP 2016*, pp. 30–35, 2016, doi: 10.1109/TENCONSpring.2016.7519373

[1] N. Hassan, K. L. A. Yau, and C. Wu, “Edge computing in 5G: A review,” *IEEE Access*, vol. 7. Institute of Electrical and Electronics Engineers Inc., pp. 127276–127289, 2019. doi: 10.1109/ACCESS.2019.2938534.

[2] S. Singh, A. Kumar Singh, Karunesh, A. Pandey, and R. Singh, “A Novel MIMO Microstrip Patch Antenna for 5G Applications,” in *Proceedings - IEEE 2021 International Conference on Computing, Communication, and Intelligent Sistems, ICCCIS 2021*, Institute of Electrical and Electronics Engineers Inc., Feb. 2021, pp. 828–833. doi: 10.1109/ICCCIS51004.2021.9397137.

[3] S. Parkvall, E. Dahlman, A. Furuskar, and M. Frenne, “NR: The new 5G radio access technology,” *IEEE Communications Standards Magazine*, vol. 1, no. 4, pp. 24–30, Dec. 2017, doi: 10.1109/MCOMSTD.2017.1700042.

[4] A. S. Mirfananda and M. Suryanegara, “5G spectrum candidates beyond 6 GHz: A simulation of Jakarta environment,” *Proc. - 2016 IEEE Reg. 10 Symp. TENSYMP 2016*, pp. 30–35, 2016, doi: 10.1109/TENCONSpring.2016.7519373

[5] A. Hikmaturokhman, K. Ramli, and M. Suryanegara, “Spectrum Considerations for 5G in Indonesia,” *Proceeding - 2018 Int. Conf. ICT Rural Dev. Rural Dev. through ICT Concept, Des. Implic. IC-ICTRuDEv 2018*, pp. 23–28, 2018, doi: 10.1109/ICICTR.2018.8706874.

[6] A. M. Raharjo, Z. Maryam, and R. Hakimi, “Spectrum analysis of 5G initial deployment for Indonesia,” in *Proceeding of 14th International Conference on Telecommunication Sistems, Services, and Applications, TSSA 2020*, Institute of Electrical and Electronics Engineers Inc., Nov. 2020. doi: 10.1109/TSSA51342.2020.9310821.

[7] M. Clenet, C. B. Ravipati, and L. Shafai, “Bandwidth enhancement of U-slot microstrip antenna using a rectangular stacked patch,” *Microwave and Optical Technology Letters*, vol. 21, no. 6, pp. 393–395, Jun. 1999, doi: 10.1002/(sici)1098-2760(19990620)21:6

[8] H. Al-Saif, M. Usman, M. T. Chughtai, and J. Nasir, “Compact Ultra-Wide Band MIMO Antenna Sistem for Lower 5G Bands,” *Wirel Commun Mob Comput*, vol. 2018, 2018, doi: 10.1155/2018/2396873.

[9] Y. Y. Liu, X. Y. Zhang, and S. J. Yang, “Compact dual-band dual-polarized filtering antenna for 5G base station applications,” in *2020 International Symposium on Antennas and Propagation, ISAP 2020*, Institute of Electrical and Electronics Engineers Inc., Jan. 2021, pp. 791–792. doi: 10.23919/ISAP47053.2021.9391214.

[10] W. Zhang, Z. Weng, and L. Wang, “Design of a dual-band MIMO antenna for 5G smartphone application,” in *2018 International Workshop on Antenna Technology (iWAT)*, 2018, pp. 1–3. doi: 10.1109/IWAT.2018.8379211.

[11] Y. Li, Z. Zhao, Z. Tang, and Y. Yin, “Differentially Fed, Dual-Band Dual-Polarized Filtering Antenna with High Selectivity for 5G Sub-6 GHz Base Station Applications,” *IEEE Trans Antennas Propag*, vol. 68, no. 4, pp. 3231–3236, Apr. 2020, doi: 10.1109/TAP.2019.2957720.

[12] W. S. Chen and Y. C. Lin, “Design of 2×2 microstrip patch array antenna for 5G C-band access point applications,” in *2018 IEEE International Workshop on Electromagnetics: Applications and Student Innovation Competition, iWEM 2018*, Institute of Electrical and Electronics Engineers Inc., Nov. 2018. doi: 10.1109/iWEM.2018.8536673.

[13] G. B. Wiryawan, K. Fayakun, H. Ramza, M. A. Zakariya, E. Roza, and D. A. Cahyasiwi, “ Hairpin Antenna-Filter with Enhanced Gain for 5G Applications,” *Jurnal Rekayasa Elektrika*, vol. 18, no. 4, Dec. 2022, doi: 10.17529/jre.v18i4.27754.

[14] D. PARAGYA and H. SISWONO, “3.5 GHz Rectangular Patch Microstrip Antenna with Defected Ground Structure for 5G,” *ELKOMIKA: Jurnal Teknik Energi Elektrik, Teknik Telekomunikasi, & Teknik Elektronika*, vol. 8, no. 1, p. 31, Jan. 2020, doi: 10.26760/elkomika.v8i1.31.

[15] A. P. Prakusya, D. A. Nurmantris, and R. A. -, “ 4 Element MIMO Antenna For 5G Communications at 3.5 GHZ Frequency,” *Jurnal Rekayasa Elektrika*, vol. 18, no. 3, Sep. 2022, doi: 10.17529/jre.v18i3.26673.

[16] R. GANDARRITYAZ, M. F. E. PURNOMO, and F. H. PARTIANSYAH, “ Design, Optimization and Analysis of High Isolation Dual-Band MIMO 5G Antenna for Smartphone Implementation,” *ELKOMIKA: Jurnal Teknik Energi Elektrik, Teknik Telekomunikasi, & Teknik Elektronika*, vol. 10, no. 4, p. 783, Oct. 2022, doi: 10.26760/elkomika.v10i4.783.

[17] H. S. Singh, B. Meruva, G. K. Pandey, P. K. Bharti, and M. K. Meshram, “LOW MUTUAL COUPLING BETWEEN MIMO ANTENNAS BY USING TWO FOLDED SHORTING STRIPS,” *Prog. Electromagn. Res. B*, vol. 53, no. May, pp. 205–221, 2013.

[18] R. Bakale, A. Nandgaonkar, S. Deosarkar, and M. Munde, “Design of Ultra-Wideband MIMO Antenna with Dual Band Elimination Characteristics and Low Mutual coupling,” *Prog. Electromagn. Res. C*, vol. 123, no. September, pp. 237–251, 2022, doi: 10.2528/PIERC22062202

.